

Interactive comment on “Glyoxal vertical columns from GOME-2 backscattered light measurements and comparisons with a global model” by C. Lerot et al.

C. Lerot et al.

christophe.lerot@aeronomie.be

Received and published: 24 November 2010

The authors gratefully thank the reviewers and the editor for their interesting comments which did contribute to improve the manuscript.

Editor's comments (R. Volkamer)

COMMENT: Page 21157, line 5: "The systematic errors on the slant column densities ($\sigma_{S,syst}$) mainly originate from uncertainties in the reference cross-section data sets and their cross-correlations. The systematic errors due to the glyoxal cross-sections have been estimated at 13%, which is the mean relative difference between the cross-sections of Volkamer et al. (2005a) and those measured by Horowitz et al. (2001)
C10193

with a lower spectral resolution." It would be helpful if the authors could separate more clearly the effect of (1) uncertainties in the reference cross-section data and (2) cross-correlations. Notably, in recording their cross section, Horowitz et al., (2001) observed deviations from Lambert-Beer's Law of up to 15%. An explanation was provided by means of high-resolution crosssection modeling (Volkamer et al., 2005a) that demonstrated this non-linear behavior is caused by the considerable ro-vibronic structure, which, when observed at low spectral resolution, results in the apparent absorption to become dependent on the column density of glyoxal. As recognized by the JPL evaluation panel 'The UV spectrum reported by Volkamer et al. is further consistent with IR spectral parameters, for which glyoxal photolysis is not a problem, and which were obtained by simultaneous recording of UV and IR spectra in identical glyoxal fillings of the absorption cell.' Notably, the UV spectrum agrees within 5% with several IR spectra, better in instances. The discussion of systematic error sources currently ignores this knowledge, which might alter the magnitude and apportionment of uncertainty.

REPLY: Thank you for this interesting comment that highlights the quality of the glyoxal cross-section data set. We have decreased the uncertainty associated to the glyoxal cross-sections from 13% to 5%. Figure 8 has been updated with new systematic and total errors. The impact of this change on systematic and total errors is relatively small, making unnecessary an update of Figs. 12 and 13. This part of the text (Page 21157, line 5) has been changed as follows:

"The systematic errors on the slant column densities ($\sigma_{S,syst}$) mainly originate from uncertainties in the reference cross-section data sets and their cross-correlations. The uncertainties associated to the glyoxal cross-sections have been estimated to be less than 5% (Volkamer et al., 2005). In addition, the uncertainties in the other cross-section data sets included in the DOAS fit also contribute to the systematic errors via their cross-correlations with the glyoxal spectrum. Their respective contributions have been..."

COMMENT: Page 21158, line 19; also Fig. 7: The authors discuss the effect of cloud factions on the AMF for "two opposite glyoxal profiles: one peaking at the surface and

the other being constant in the troposphere", but remain rather vague in terms of the actual profile shape used in these calculations (Table 2). From Figure 7, however, it appears that for both profiles most glyoxal is taken to reside above the cloud layer (top height 2km). Else, how can the authors explain that the AMF is independent of the cloud fraction? Can the authors make a more explicit case that the assumed vertical distributions are indeed 'opposed' in terms of conservatively bracketing uncertainty? How would the AMF sensitivity, and the error apportionment change if all glyoxal was indeed located in the MBL (<700m according to the authors)?

REPLY: There seems to have been some misunderstanding on this point. Let us try and clarify the AMF formulation and ghost column correction approach used in this work. One can find in the literature two slightly different approaches for the treatment of cloudy scenes in the independent pixel approximation. These approaches result in slightly different ghost column corrections.

Method 1:

In the first method, the cloudy AMF is calculated according to Eq. (1) using an integration performed from the top of atmosphere down to the ground. Accordingly, the vertical column can be calculated as $VCD = SCD / (AMF_{tot})$ where AMF_{tot} is the cloud fraction-weighted sum of the clear and cloudy AMF. In that case, the ghost column correction is implicitly accounted for in the cloudy AMF which generally decreases when the cloud fraction increases (as expected by the reviewers).

Method 2:

The second method, which has been used in this work, uses an absolute correction for the ghost column as described e.g. in Van Roozendael et al. (JGR, 2006). In this case, the integration to calculate the cloudy AMF is performed down to the cloud top height instead of to the ground. Calculated in this way, the total AMF shows the behaviour displayed in Figure 7, which is weakly dependent on the a-priori profile shape and cloud-top altitude. According to this formulation, a ghost column term (GC) has to be explicitly added to the slant column and the vertical column is now calculated as

C10195

$$VCD = (SCD + GC) / AMF_{tot}.$$

It can be demonstrated that both approaches give similar results for a given a priori profile. We have selected the second one because we found it more stable. Indeed, the total AMF calculated using the method (1) tends to be close to 0 for cloudy pixels and the VCD tends to become unreliable (because of the noise, the SCD in cloudy conditions can strongly differ from 0). In addition, the method (1) appears to be more sensitive to profile shape uncertainties than method (2).

To clarify this in the manuscript, we have replaced the first paragraph of page 21156 by the following text:

Cloud contamination of pixels usually prevents probing the lower tropospheric part of the atmosphere with spaceborne instruments. Therefore, a cloud correction based on the independent pixel approximation (Martin et al., 2002) is applied to calculate the glyoxal vertical columns. The VCD computation is based on the formulation given e.g. in Van Roozendael et al. (2006):

$$VCD = \frac{SCD + \Phi GC A_{cloud}}{(1 - \Phi)A_{clear} + \Phi A_{cloud}} = \frac{SCD + \Phi GC A_{cloud}}{A_{tot}}, \quad (1)$$

where Φ is the intensity-weighted cloud fraction, GC is the so-called ghost column accounting for the glyoxal column shielded by the cloud and calculated using the a priori profiles. A_{clear} and A_{cloud} are respectively the air mass factors for the clear and cloudy parts of the pixel calculated using Eq. (1) where the integration is performed down to the ground or to the cloud top height. The cloud parameters are provided by the FRESCO+ cloud algorithm (Wang et al., 2008), that retrieves the effective cloud fraction and cloud top height assuming a Lambertian cloud with an albedo of 0.8. Although no explicit correction for aerosols is applied, the cloud algorithm implicitly accounts for a possible contribution from reflecting aerosols by retrieving higher effective cloud fractions (Boersma et al., 2004). In addition, Leitao et al. (2010) found that neglecting aerosols leads to moderate errors in most cases. However, these errors might be

C10196

more important in case of high absorbing aerosol content during large biomass burning events or in heavily polluted megacities and need to be further investigated.

Also, Equation (2) has been updated accordingly. Figure 7 has been improved by adding an insert representing the profiles used for the AMF calculations and the caption has been completed.

COMMENT: Page 21162, line 28: "Assuming a uniform glyoxal concentration in the marine boundary layer ($z < 700$ m, based on ECMWF analyses), the vertical column densities corresponding to these ship measurements reach 3×10^{14} molec/cm², consistent with our glyoxal observations from GOME-2 and those from SCIAMACHY (Vrekoussis et al., 2009)." How is a boundary layer profile (up to 700m, according to the authors) consistent with Figure 7? Some explanation would be helpful how the argument about vertical glyoxal distributions, and apparent agreement with the MBL profile supported by the ship measurements are internally consistent. Wouldn't a MBL profile of glyoxal be shielded for the view from space at the higher cloud fractions? It would help if the authors could include a figure that shows the vertical distributions assumed in their retrievals (substitute for Table 2), and bind uncertainty in terms of unmeasured vertical distributions in a consistent and conservative error analysis that reflects our current knowledge, or - unless supported by measurements - lack thereof.

REPLY: This comment is strongly related to the previous one and has been mostly answered above. As mentioned in the paper, the uncertainties associated to the a priori profiles are large, especially above oceans where the glyoxal production mechanisms are not understood. This is the reason why larger uncertainties have been considered for oceanic regions than for lands in the error computation. We would prefer keeping table 2 to illustrate this. An example of glyoxal profile is now given in Fig. 7. It can also be seen from Fig. 8 that the AMF error due to the profile shape strongly decreases with cloud contamination and is already very small for cloud fraction equal to 0.1. The error due to the ghost column correction (also due to profile shape uncertainties) significantly increases at high cloud fractions. As mentioned in page 21159, "*it is recommended not*

C10197

to use the pixels strongly contaminated by clouds as their associated measured column is mostly influenced by the a priori information via the ghost column correction, especially for scenes containing high-altitude clouds. In practice, we filter out all pixels with a cloud fraction larger than 40%, this threshold resulting from a trade-off between number of measurements and limited cloud contamination. "

Considering the low AMF errors, the glyoxal measurements from oceanic pixels with cloud fraction lower than 0.4 appear to be reliable, even if their associated relative errors are more important.

C10198

Referee 2's comments

COMMENT:

page 21152 line 2/Table 1: The HITRAN data base was updated 2008 leading to significant improvements. Why didn't the authors use a water vapor cross-section from the HITRAN 2008 data base?

REPLY: Both water vapor cross-sections from HITRAN 2004 and from HITRAN 2008 have been tested in our GOME-2 glyoxal retrievals. A stronger correlation was observed between the glyoxal and the water vapor when Hitran 2008 was used instead of Hitran 2004, this correlation leading to bias in the glyoxal SCD when the water vapor concentration is important. Therefore, we selected the data set from Hitran 2004 as a baseline. A further analysis of the impact of the water vapor spectroscopy will be performed in future.

COMMENT:

page 21153 lines 16-18: In the 405-490 nm wavelength range window, a significant NO₂ absorption can be expected. What are the reasons that no NO₂ cross-section was included? The liquid water cross-section is very broad-banded. What is the impact of the degree of the fitted polynomial to the value of the liquid water optical density?

REPLY: As mentioned by the reviewer, the liquid water cross-section is very broad-banded on contrary to the NO₂ cross-section. There is no strong cross-correlation between these two data sets making almost no difference between the retrieved liquid water with or without NO₂. This has been experimentally verified and the differences are generally very small. Nevertheless, since there is no drawback to include a NO₂ cross-section in the liquid water retrieval, we will consider it for next reprocessing of the product.

The cross-correlation between the polynomial and the liquid water is a bit more important. Test retrievals have been performed using a polynomial of degree 3 instead of 5. Over oceans, the liquid water SCD retrieved with this polynomial were on average a bit

C10199

higher, the differences being close to the SCD error. Over lands, the liquid water SCDs with this polynomial tend to move away from 0, especially over bright surfaces. Even if it is difficult to assess the appropriateness of the absolute level of liquid water SCD, the latter result indicates that our polynomial of degree 5 is better, at least over lands. A contribution to the total glyoxal column error from possible liquid water fit error has been accounted for in the error budget.

COMMENT: p. 21153 line 19: typo: "betwen" -> "between"

REPLY: Corrected.

COMMENT: Figure 5: Can the authors provide a physical explanation for the liquid water distribution shown in Fig. 5? Can the authors comment on the reliability of the glyoxal retrieval in case the distribution does not have a physical explanation?

REPLY: We have added at the end of the second paragraph of the section "Impact of liquid water absorption" the following sentence:

"These regions are characterized by a very low concentration of chlorophyll, which absorbs in the visible region. The light path below the sea surface is consequently more important there than in other oceanic regions."

COMMENT: page 21163 lines 1-2 and page 21166 lines 22-23: I agree with the editor in terms of the claimed consistency between the ship measurements and the retrieval described in this manuscript. How can a glyoxal layer in the lowest 700m be consistent with the assumed profile shape used in the retrieval?

REPLY: This has been extensively answered above. Please, see the reply to the Editor's comments

COMMENT: page 21166 lines 5-6: "In this error budget, the neglect of absorbing aerosols has not been considered." Can the authors rephrase this sentence since it is confusing?

REPLY: The sentence has been rephrased as:

"The impact of absorbing aerosols has to be further investigated, especially because of

C10200

their possible large concentrations during important fire events and in heavily polluted megacities."

Interactive comment on Atmos. Chem. Phys. Discuss., 10, 21147, 2010.

C10201

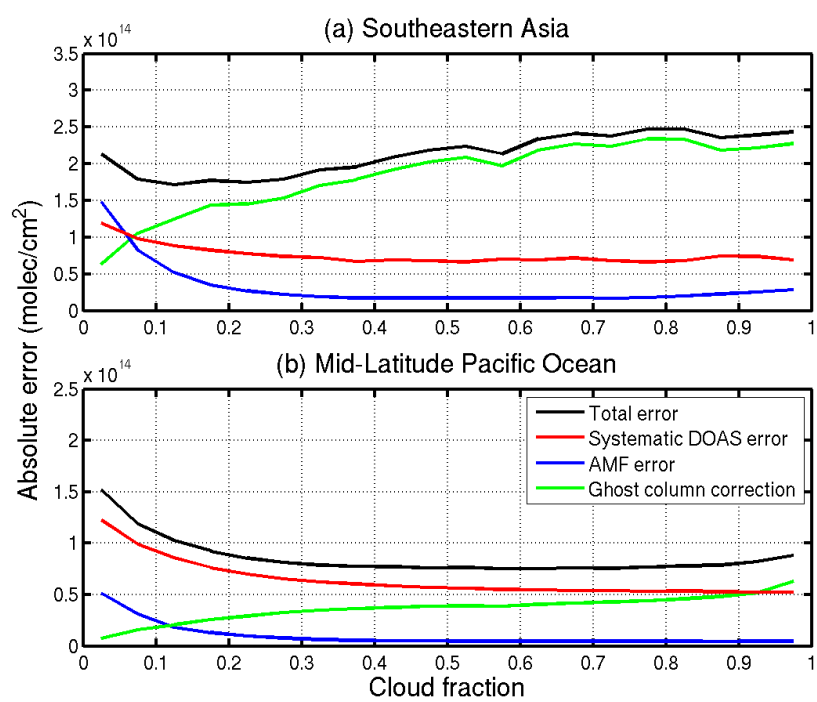


Fig. 1.

C10202

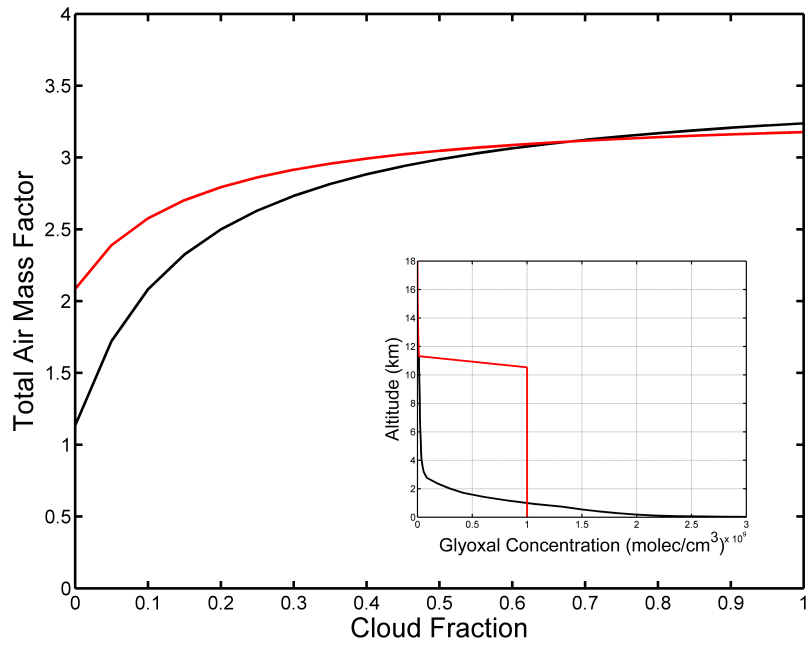


Fig. 2.

C10203